

Published in final edited form as:

Epilepsy Behav. 2013 November ; 29(2): . doi:10.1016/j.yebeh.2013.08.028.

Integration of gray matter nodules into functional cortical circuits in periventricular heterotopia

Joanna A. Christodoulou¹, Mollie E. Barnard², Stephanie N. Del Tufo¹, Tami Katzir³, Susan Whitfield-Gabrieli¹, John D.E. Gabrieli¹, and Bernard S. Chang²

¹Department of Brain and Cognitive Sciences and McGovern Institute for Brain Research, Massachusetts Institute of Technology, Cambridge, Massachusetts

²Comprehensive Epilepsy Center, Department of Neurology, Beth Israel Deaconess Medical Center and Harvard Medical School, Boston, Massachusetts

³Department of Learning Disabilities, University of Haifa, Haifa, Israel

Abstract

Alterations in neuronal circuitry are recognized as an important substrate of many neurological disorders, including epilepsy. Patients with the developmental brain malformation of periventricular nodular heterotopia (PNH) often have both seizures and dyslexia, and there is evidence to suggest that aberrant neuronal connectivity underlies both of these clinical features. We used task-based functional MRI (fMRI) to determine whether heterotopic nodules of gray matter in this condition are integrated into functional cortical circuits. Blood oxygenation level-dependent (BOLD) fMRI was acquired in eight participants with PNH during the performance of reading-related tasks. Evidence of neural activation within heterotopic gray matter was identified, and regions of cortical co-activation were then mapped systematically. Findings were correlated with resting-state functional connectivity results and with performance on the fMRI reading-related tasks. Six participants (75%) demonstrated activation within at least one region of gray matter heterotopia. Cortical areas directly overlying the heterotopia were usually co-activated (60%), as were areas known to have functional connectivity to the heterotopia in the task-free resting state (73%). Six of seven (86%) primary task contrasts resulted in heterotopia activation in at least one participant. Activation was most commonly seen during rapid naming of visual stimuli, a characteristic impairment in this patient population. Our findings represent a systematic demonstration that heterotopic gray matter can be metabolically coactivated in a neuronal migration disorder associated with epilepsy and dyslexia. Gray matter nodules were most commonly coactivated with anatomically overlying cortex and other regions with resting-state connectivity to heterotopia. These results have broader implications for understanding the network pathogenesis of both seizures and reading disabilities.

Keywords

malformation; migration; epilepsy; dyslexia; connectivity

© 2013 Elsevier Inc. All rights reserved.

Corresponding author: Bernard S. Chang, M.D., Comprehensive Epilepsy Center, E/KS-457, Beth Israel Deaconess Medical Center, 330 Brookline Ave, Boston, MA 02215, phone 617-667-2889; fax 617-667-7919, bchang@bidmc.harvard.edu.

Publisher's Disclaimer: This is a PDF file of an unedited manuscript that has been accepted for publication. As a service to our customers we are providing this early version of the manuscript. The manuscript will undergo copyediting, typesetting, and review of the resulting proof before it is published in its final citable form. Please note that during the production process errors may be discovered which could affect the content, and all legal disclaimers that apply to the journal pertain.

1. Introduction

Aberrant neuronal circuitry is recognized as an important underlying substrate of epilepsy and other neurological disorders [1,2]. For example, in mesial temporal sclerosis, one of the most common pathologies seen in focal epilepsy in adults, aberrant sprouting of axons from hippocampal dentate granule cells has been identified and may play a role in epileptogenesis [3,4]. Similarly, one of the most prevalent learning disabilities in the general population, dyslexia, has been associated with defects in cortico-cortical tracts through the cerebral white matter, and these circuit changes may be the underlying anatomical basis for difficulties with reading fluency [5].

The unique developmental brain malformation of periventricular nodular heterotopia (PNH) has served as a model disorder for aberrant circuitry in neurological disease [6,7]. The disorder is characterized anatomically by nodules of misplaced gray matter that line the walls of the lateral ventricles; in the classic diffuse form of PNH, the nodules are bilateral and often so numerous as to be confluent [8]. The most commonly identified genetic cause of bilateral diffuse PNH is a null mutation in the *FLNA* gene, which encodes a cytoskeletal actin-binding protein, and the developmental defect appears to involve a disruption in radial neuronal migration from the ventricular zone outward toward the cortical plate [9].

One of the remarkable clinical features of PNH is that most patients with this disorder have average cognitive abilities, despite the striking change in gray matter architecture [8]. However, a majority of individuals with PNH have a singular form of dyslexia in which reading fluency is the primary deficit, and not phonological awareness (which is impaired in most individuals with developmental dyslexia) [10]. Interestingly, the degree of white matter microstructural integrity loss in PNH, presumably caused by the presence of the periventricular nodules, correlates with the degree of reading dysfluency, likely because critical cortico-cortical tracts required for fluent processing of visual stimuli are disrupted [11].

There also is growing evidence that aberrant circuitry in PNH is associated with the epilepsy that clinically characterizes this condition. EEG spike-triggered fMRI acquisition has shown that heterotopia and overlying cortex can be simultaneously active in association with interictal epileptiform discharges [12]. We have previously shown that there is widespread aberrant structural and functional connectivity between heterotopia and overlying cortex in patients with PNH and that the degree of aberrant functional connectivity is greater among those with longer durations of epilepsy [13]. This work suggests a link between the process of aberrant circuit formation and the process of epilepsy progression over time.

In this study, we sought to use task-based fMRI in a cohort of participants with PNH to establish the neural basis of reading-related tasks in this disorder, since reading skills are selectively impaired in this population. In particular, we hypothesized that regions of periventricular gray matter heterotopia are integrated into functional circuits with overlying cortex and contribute to the behavioral reading characteristics of PNH.

2. Material and Methods

2.1. Participant selection

Participants with PNH were drawn from a cohort of individuals who had participated in a prior connectivity imaging study of this disorder [13]; all participants had been recruited from a research database of patients with malformations of cortical development, from a clinical database of patients with epilepsy at our institution, and through research referrals from clinical neurologists. Patients with a neuroimaging-confirmed diagnosis of PNH based

on the presence of at least two visible nodules of heterotopic gray matter adjacent to the lateral ventricle, each seen on more than one plane of sequence and on at least two consecutive images in one of those planes, were eligible to be enrolled. Those with prior brain surgery, inability to tolerate MRI, or a specific MRI contraindication as set forth in standard protocols of our institutions were excluded, as were pregnant women because of a lack of definitive information on fetal safety in MRI. All participants were required to be native English speakers and have an intelligence quotient > 70 in order to participate. All participants were right-handed [14].

Participants completed a behavioral testing session at the Massachusetts Institute of Technology (MIT) and an MRI scanning session at the Athinoula A. Martinos Imaging Center, McGovern Institute for Brain Research at MIT. Written informed consent was obtained from all participants in accordance with research protocols approved by the institutional review boards of Beth Israel Deaconess Medical Center and the Massachusetts Institute of Technology.

2.2. Reading-related tasks

Participants were asked to complete the following tasks inside the MRI scanner for blood oxygenation level-dependent (BOLD) signal acquisition; tasks were chosen based on well-recognized components of reading ability previously described in the dyslexia fMRI literature [15–18] and the known cognitive characteristics of the PNH patient population [11]. Participants practiced each paradigm before the scanning session. During this training period, participants listened to the same directions that were presented before completing each task in the scanner. The practice session included one trial of each condition from each task. In the scanner, the button box was in the participant's right hand. Before beginning the scan, participants were reminded to remain as still as possible for the duration of the scan to prevent head motion. All the stimuli were visually presented in white font on a black background on a rear-projection screen via PsychToolBox software [19,20]. The screen size, zoom, and focus were calibrated for each participant to ensure that the entire visual field of the projected images was visible through the mirror mounted on the head coil.

2.2.1. Phonological—Participants completed print-mediated and picture-mediated phonological tasks that shared the same task demands but differed in the stimulus sets. Participants were presented visually with two words (print-mediated) or two line drawings (picture-mediated) simultaneously, and were asked to indicate by button press whether the two stimuli matched (words were identical or drawings showed the same object) or whether the two stimuli rhymed. As a control condition, participants were presented visually with two sets of angled vertical lines (slash marks) and asked to indicate whether the two sets of stimuli matched. As a baseline condition, participants viewed a fixation cross for which no action was required. Accuracy and reaction time were measured.

The stimuli were matched based on the following criteria: written frequency, verbal frequency, number of letters, number of phonemes, number of syllables, and concreteness. The picture-mediated phonological task's stimuli were monochromatic image pairs on a black background. Specifically, the participants were instructed to determine matching or rhyming based on the word of the object the picture represented. For example, in a matched set, the picture pairs would both depict the same object, but the pictures themselves would be distinct representations of the item.

Each trial lasted 4 seconds, with 5 trials per block. Preceding each block was a 2 second instructional cue indicating whether the block would be a match or rhyme condition. Rest blocks showing a white fixation cross had a duration of 20 seconds per block. Each participant completed one run for each phonological task (print or picture-mediated). Each

run consisted of 30 trials per condition, with the total duration of the rest condition equaling the duration of a single condition.

2.2.2. Orthographic—Participants were presented visually with two words, two strings consisting of symbols (Arabic written language characters), or two sets of angled vertical lines ($\setminus /$), and were asked to indicate by button press whether the two stimuli matched. The control condition consisted of visual fixation on a cross. Accuracy and reaction time were measured.

Each stimuli pair was presented for 2.5 seconds and then followed by a question mark for 1.5 seconds for a total of 4 seconds per trial, with four trials per block. Rest conditions showing a white fixation cross lasted for 16 seconds. Each participant completed one run, consisting of 24 trials per condition, with the total duration of the rest condition being equal to the duration of a single condition.

2.2.3. Rapid automatized naming (RAN)—Participants were presented with a 10×5 matrix of letters, numbers, or alternating letter-number stimuli (2-set). Rapid naming letter cards were adapted from the stimuli used by Misra et al. [17] and from the clinical RAN/RAS tool of rapid naming by Wolf and Denckla [21]. A series of numbers (2, 4, 6, 7, 9) were randomly organized into seven matrices for the rapid naming number condition. The 2-set rapid naming cards were created using randomly generated sequences of the same stimuli (a, d, o, p, s; 2, 4, 6, 7, 9) for seven matrices.

Participants were asked to name each individual item to themselves silently, from left to right, top to bottom, as quickly as possible without making mistakes, pressing a button to indicate completion of each line. Compliance and accuracy were not measured as the task was performed silently, but the time for completion of each line was recorded. The control condition consisted of visual fixation on a 10×5 matrix of crosses. The paradigm was presented using a blocked design with one card per block and seven blocks per condition (three rapid naming conditions).

2.3. Imaging acquisition

Imaging was performed using a Siemens 3T MAGNETOM Trio Tim System with a commercial 12-channel matrix head coil (Siemens Medical Solutions, Erlangen, Germany). To minimize movement, tetrahedron-shaped foam pads were placed between the coil and either side of the participant's head.

Sagittal localizer scans were aligned to a multi-subject atlas to derive automatic slice prescription for consistent head position across participants. High-resolution structural whole-brain images were acquired using a T1-weighted magnetization-prepared rapid-acquisition gradient-echo (MPRAGE) sagittal anatomical sequence (128 slices per slab, 256×256 matrix, 256 mm field of view (FOV), 1.33 mm slice thickness, 0.63 mm interslice gap, TR = 2530 ms, TI = 1100 ms, TE = 3.39 ms, flip angle = 7 degrees).

Functional data were collected in an ascending interleaved acquisition using a continuously-sampled gradient echo T2*-weighted EPI sequence sensitive to BOLD contrast. The gradient-echo EPI images were acquired with PACE, an online motion correction algorithm that minimizes movement-related artifact by adjusting the system gradients and the acquisition FOV between one whole brain acquisition and another for head movement [22]. Thirty-two sagittal slices parallel to the anterior commissure-posterior commissure (AC-PC) line were imaged providing whole brain coverage (voxel size $3.1 \times 3.1 \times 4.0$ mm, 64×64 mm matrix, 200 mm FOV, 4 mm slice thickness, 0.8 mm interslice gap, TR = 2000 ms, TE = 30 ms, flip angle = 90° , bandwidth = 2298 Hz/Px, echo spacing = 0.5 ms). At the

beginning of each functional scan, five additional images (10 second duration) were discarded to allow for T1 equilibration. One functional run was collected for each phonological task (258 volumes, 8:46 minutes), orthographic task (245 volumes, 8:18 minutes), and RAN task (224 volumes, 7:38 minutes).

2.4. Imaging data analysis

Cortical reconstruction and parcellation of anatomical images were performed using Freesurfer v5.1.0 (<http://surfer.nmr.mgh.harvard.edu>). Functional data preprocessing and statistical analysis were performed using statistical parametric mapping software (SPM8; Wellcome Department of Cognitive Neurology, London, UK; <http://www.fil.ion.ucl.ac.uk/spm/software/spm8>) using workflows in Nipype v0.5 (<http://nipype.org/nipype>) [23]. Functional data were slice time corrected using the first slice as the reference. Motion correction of the functional timeseries was achieved via six degree-of-freedom rigid-body affine transformation with trilinear interpolation to align each slice to the mean functional volume using the algorithm in SPM8. Data were not spatially normalized due to the unique anatomical pattern of gray matter heterotopia in each participant. Images were spatially smoothed using a Gaussian filter (4-mm full width at half maximum) to decrease uncorrelated spatial noise. For each participant, the mean functional volume and the T1-weighted structural image were co-registered via six degree-of-freedom rigid-body affine transformation with trilinear interpolation using *bbregister* with FSL affine initialization optimized for T2 weighted images [24].

First-level analyses were performed in participant-native space due to unique heterotopia anatomy. The stimuli for each imaging task were modeled as box-car functions with widths equal to block durations and convolved with the canonical hemodynamic response function from SPM8. A high-pass filter (cutoff = 128s) was used on the model to reduce the impact of physiological noise. Outlier image volumes in the BOLD time series were identified using ART (www.nitrc.org/projects/artifact_detect) based on either the mean intensity of image volume greater than 3 standard deviations from the mean intensity of the time series or composite head motion greater than 1 mm, based on scan-to-scan movement. Data were analyzed using a fixed effects model that accounted for motion effects by regressing the six motion parameters (x, y, z, pitch, roll, yaw) for each individual by task, and included outlier scans as nuisance regressors (i.e., covariates which consist of all zeros and a one for the artifactual time point). A voxel-wise threshold of $p < 0.05$ (cluster-wise false discovery rate corrected for multiple comparisons at $p < 0.05$) and a cluster extent of 10mm³ or more voxels were used to detect significant individual activations for each contrast. Functional image volumes were masked to include only brain voxels based on an anatomical mask created by binarizing and dilating by one voxel the FreeSurfer *aparc+aseg.mgz* volume transformed from each individual's anatomical to functional space.

The Freeview module of the Freesurfer suite was then used to identify all instances in which significant BOLD activation overlapped with manually outlined regions of interest (ROIs) representing the heterotopic nodules. For each task contrast in each participant in which heterotopia activation was identified, the regions of cerebral cortex that showed co-activation with heterotopia were catalogued according to a previously described anatomical scheme and compared with cortical regions previously shown to share resting-state functional connectivity with the heterotopia in question [13].

2.5. Imaging artifact detection

The percentage of images identified as outliers, based on intensity or motion, was minimal. The mean percentage of images identified as intensity outliers out of the total number of images acquired were as follows by task: phonological print-mediated ($M=0.48\%$,

$SD=0.50\%$), phonological picture-mediated ($M=0.78\%$, $SD=0.78\%$), orthographic ($M=0.56\%$, $SD=0.69\%$), RAN ($M=0.67\%$, $SD=0.41\%$). The mean percentage of images identified as motion outliers out of the total number of images acquired were as follows by task: phonological print-mediated ($M=0.87\%$, $SD=2.47\%$), phonological picture-mediated ($M=1.26\%$, $SD=3.41\%$), orthographic ($M=0.26\%$, $SD=0.37\%$), RAN ($M=0.56\%$, $SD=1.14\%$).

2.6. Imaging-behavioral analyses and statistical methods

Performance scores on behavioral tasks and the relationships between functional imaging results and behavioral performance were analyzed using InStat software (GraphPad, La Jolla, CA) and SPSS Statistics software (IBM, Armonk, NY). Statistical significance was assessed at a threshold of $\alpha = 0.05$ for all comparisons.

3. Results

3.1. Participant characteristics and task performance

Eight PNH participants (six female), all of whom had a history of complex partial seizures and an identified impairment in reading fluency, were enrolled (mean age 29.6 years, range 19–42). Detailed demographic, cognitive, radiological, and clinical epilepsy-related characteristics of these participants have been previously reported [11,13].

Repeated-measures analysis of variance (ANOVA) was used to analyze results for accuracy and reaction time for each task, followed by post-hoc comparisons for significant main effects. (See Table 1 for means and standard deviations.) For the print-mediated phonological task (print word rhyming, print word matching, line matching), participant accuracy scores ($F(2, 14) = 7.707$, $p < 0.006$) and reaction times ($F(2, 14) = 6.194$, $p = 0.012$) differed significantly across conditions. Post-hoc comparisons for the print-mediated phonological task showed highest accuracy for word matching, and shorter reaction times for word matching as compared to line matching. The picture-mediated phonological task (picture word rhyming, picture word matching, line matching), showed significant accuracy ($F(2, 6) = 19.90$, $p = 0.002$) and reaction time differences ($F(2, 14) = 26.773$, $p = 0.000016$) as well. Post-hoc comparisons for the picture-mediated phonological tasks showed highest accuracy for word matching as compared to both word rhyming and line matching, and longest reaction times for word rhyming as compared to both other conditions. On the orthographic tasks, accuracy was comparable across conditions ($F(3,21) = 1.728$, $p = 0.192$), but reaction time differences ($F(3,21) = 12.835$, $p = 0.000055$) were driven by fastest word matching performance as compared to all other conditions. RAN task performance differences ($F(2, 14) = 10.053$, $p = 0.002$) were driven by slower performance on the two-set condition as compared to letter and number conditions.

3.2. Heterotopia activation in association with reading-related tasks

Robust BOLD activation was seen in all participants across our panel of tasks, particularly in contrasts involving an active task condition compared to a visual fixation control condition. In order to ensure the specificity of activation and test the hypothesis that heterotopic gray matter is integrated into discrete functional circuits, we analyzed seven primary task contrasts, chosen to highlight core components of reading ability (based on prior fMRI studies) and specific aspects of reading fluency, a known impairment in this patient cohort.

Six of eight (75%) participants with PNH showed evidence of significant BOLD activation within at least one region of gray matter heterotopia (either entirely within or substantially overlapping a heterotopic nodule) in association with at least one of the seven primary task

contrasts (Table 2). In five participants, multiple tasks elicited heterotopia activation. In three participants, differing heterotopic nodules were activated during different tasks.

Among the seven primary task contrasts, six (86%) elicited heterotopia activation within at least one participant. The two task contrasts with the largest number of examples of heterotopia activation (four participants each) were rapid number naming and rapid two-set naming, while rapid letter naming was associated with such activation in two participants. The phonological task contrast of picture-mediated word rhyming vs. word matching also elicited heterotopia activation within two participants.

In total, 15 instances of heterotopic gray matter activation were seen, and in all cases simultaneous co-activation within discrete regions of cerebral cortex was seen. In nine instances (60%), cortex directly overlying the heterotopic nodule was co-activated. In 11 instances (73%), co-activated regions of cortex (whether directly anatomically overlying or not) included those that had previously been demonstrated to have functional connectivity to the activated heterotopic nodule in resting-state BOLD imaging [13].

3.2.1. Heterotopia activation in association with phonological tasks—The contrast of the picture-mediated word rhyming task and word matching task, which highlights the neural basis of phonological processing, demonstrated BOLD activation within heterotopic gray matter in two out of eight participants. Activation was seen within a nodule of gray matter along the posterior wall of the left lateral ventricle in Participant 2 (Table 2, Figure 1A). Co-activation was seen within multiple regions of ipsilateral and contralateral cortex, particularly in the frontal lobes; one of these regions had been shown previously to have functional connectivity to that specific nodule in the resting state. Participant 4 demonstrated activation within a right anterior heterotopic nodule in this task contrast, with co-activation within overlying cortex and a region of contralateral posterior cortex (Figure 1B). The contrast of the print-mediated word rhyming task and word matching task did not show evidence of heterotopia activation in any participants.

3.2.2. Heterotopia activation in association with orthographic tasks—Two of eight participants demonstrated heterotopia activation for tasks of orthographic processing. The contrast of the word-matching task and the line-matching task, which highlights the neural basis of orthographic processing, demonstrated BOLD activation within a nodule of gray matter heterotopia along the anterior wall of the left lateral ventricle in Participant 1 (Table 2, Figure 2A). Co-activation was seen within a region of overlying cortex in the left frontal lobe. The contrast of the word-matching task and the symbol-matching task, which also highlights orthographic processing, demonstrated BOLD activation within a right anterior heterotopic nodule in Participant 5 (Figure 2B), with co-activation of multiple bilateral cortical regions, including those that had been shown to have resting-state functional connectivity to that specific nodule previously. These contrasts did not show evidence of heterotopia activation in the other participants.

3.2.3. Heterotopia activation in association with RAN tasks—Five of eight participants demonstrated heterotopia activation for RAN tasks. The contrast between the rapid letter naming task and a rest condition with visual fixation demonstrated BOLD activation within a right anterior heterotopic nodule in Participant 4 (Table 2, Figure 3A). Co-activation was seen within overlying right frontal cortex and a discrete region of homologous contralateral cortex, two regions that had been shown to have resting-state functional connectivity to that nodule previously. A similar pattern of activation was seen in this participant with rapid number naming and rapid two-set naming as well. The rapid letter naming contrast also demonstrated activation within a left posterior nodule in Participant 2, with co-activation seen in overlying cortex and multiple other regions. With rapid number

naming and rapid two-set naming, Participant 6 (Figure 3B) and Participant 7 demonstrated activation within regions of periventricular heterotopia, as well as within multiple regions of cortex bilaterally. With rapid 2-set naming, Participant 1 demonstrated activation within a right anterior nodule, as well as overlying cortex and multiple other cortical regions (Figure 3C).

4. Discussion

Here we report a systematic investigation of the functionality of heterotopic gray matter in the unique developmental brain malformation of PNH, a model condition for the study of aberrant neural circuitry and its contribution to epilepsy and reading difficulties. Using a panel of reading-related behavioral tasks chosen because of the known deficits in patients with this disorder, we found evidence of functional activation within periventricular nodules across multiple participants using multiple types of tasks. In most instances of heterotopia activation, regions of overlying cortex (and often contralateral homologous cortex) were co-activated with the deep nodules, and these were usually cortical regions that had already been shown to have resting-state functional connectivity to the specific nodules in question. Aberrant heterotopia activation was seen more commonly in association with tasks shown to be more challenging in this patient population.

We previously demonstrated that there is aberrant structural connectivity and resting-state functional connectivity between periventricular heterotopic nodules and overlying regions of cerebral cortex [13], and others have demonstrated, in isolated instances, BOLD evidence of co-activation between gray matter heterotopia and cortex during the performance of particular functional tasks [25] or in association with interictal epileptiform discharges on EEG [12]. The current study goes further in demonstrating that standard behavioral tasks representing key components of a ubiquitous language function (reading) are associated with activation of heterotopia across multiple anatomical locations in multiple participants using a strict statistical threshold. This evidence that heterotopia are integrated into functional cortical circuits represents an important advance in our understanding of how neuronal migration disorders affect physiological cerebral function.

Our use of reading-related functional tasks is based on the specific behavioral phenotype that has been noted in patients with PNH, and in particular the singular defect in reading fluency seen in this disorder [11]. Our findings raise the possibility that the altered neural basis of these tasks, including the activation of periventricular nodules, is causally associated with the reading fluency deficits seen in this disorder. Indeed, the most common examples of aberrant activation occurred with tasks involving RAN, a skill which represents the cardinal impairment seen in patients with PNH-associated reading disability, as well as the task involving picture-mediated word rhyming, on which our participants showed the lowest accuracy and longest reaction times among the binary judgment tasks. However, whether active neurons within the heterotopia might serve adaptive or compensatory roles in such behavioral tasks, rather than maladaptive or pathological roles, cannot be answered by these methods; it is not known, for example, whether regions of heterotopia and cortex that are co-active have an excitatory or inhibitory relationship with each other.

There is evidence in the literature regarding the patterns of neural activation seen during the performance of tasks representing elemental components of reading. For example, orthographic tasks involving word matching have typically been linked to preferential activation within bilateral ventral posterior brain regions, but in particular a left occipitotemporal region now known as the visual word form area [26,27]. By contrast, tasks involving word rhyming and other processes that invoke predominantly phonological skills are associated with activation within a more dorsal system that includes the perisylvian

cortex and left inferior frontal gyrus [18,28]. Finally, RAN tasks appear to recruit a network of cortical regions located in both ventral and dorsal reading systems [17].

In individuals with developmental dyslexia, diverse and in some cases conflicting reading-related fMRI data have given support to a number of competing theories regarding the neurobiological basis of reading disability [29]. Our results here demonstrate that unique developmental anomalies of cerebral anatomy can lead to distinct functional alterations that are associated with a form of dyslexia. Notably, there was no consistent association between the anatomical location of the activated regions of heterotopia or cortex and the type of reading-related task during which such aberrant circuit activation was seen, supporting previous volumetric evidence that the neural correlates of these and other cognitive functions may be different in the setting of neuronal migration failure [30].

There are a number of limitations to our work. First, although PNH represents a model brain disorder for aberrant neuronal circuitry in epilepsy and reading disability, its uniqueness may restrict the broader applicability of our findings. However, there is growing evidence that many other forms of focal epilepsy, even acquired in origin (such as after traumatic brain injury), are associated with the progressive development of aberrant connectivity [31]. The standard interpretation of BOLD signal activation may be inappropriate in the setting of a cortical malformation given the possibility of altered venous drainage [32], but this appears unlikely to affect discrete periventricular nodules, as opposed to large regions of schizencephaly or polymicrogyria. By its nature, the use of task-based fMRI limits our ability to test the broad hypothesis that heterotopia are integrated into any functional circuits, since the specific tasks assessed do not represent the range of mappable functions across the cortex. Nevertheless, the fact that even with these limited tasks, discrete examples of heterotopia co-activation with cortex were seen across multiple participants, suggests that functional integration of heterotopia occurs regularly and not just in isolated circumstances [25,33]. The interpretation of BOLD fMRI can also be limited when behavioral performance on a task is suboptimal. The demonstration of heterotopia activation in the attempted performance of these reading-related tasks, whether successful or not, though, is still consistent with the notion that functional integration of the heterotopia could be either compensatory or maladaptive. Finally, the variability in robustness of BOLD activation in fMRI limits the definitiveness of our conclusions about the relationship of heterotopia activation to task performance, since the “background” level of activation is not constant across participants or across tasks.

Our findings have implications for our broader understanding of other forms of developmental brain anomalies and indeed disorders of epilepsy and cognition more generally. The notion that developmental dyslexia at its heart may be a disorder of cortical dysplasia and aberrant neuronal circuits has its origins in pathological studies of dyslexia from decades ago [34]. With increasing recognition of the importance of comorbid learning difficulties in epilepsy patients [35], our results provide additional support for the idea that functionally altered neural circuits may be a common mechanism that underlies both a tendency toward seizures and an impairment in cognitive function. In the future, tailored therapeutic options targeted toward defects of aberrant connectivity may hold promise in the treatment of both epilepsy and some of its associated comorbidities.

Acknowledgments

We thank our participants and their families for their participation, without which this study could not have been completed. We thank Tyler Perrachione, Jack Murtagh, and Kelly Halverson for assistance. Scanning was conducted at the Athinoula A. Martinos Imaging Center at McGovern Institute for Brain Research, MIT. BSC was supported by the National Institutes of Health/National Institute of Neurological Disorders and Stroke (R01 NS073601), the Epilepsy Foundation, and the William F. Milton Fund of Harvard University.

References

1. Scharfman HE. The neurobiology of epilepsy. *Curr Neur Neurosci Rep*. 2007; 7:348–54.
2. Badawy RAB, Harvey AS, Macdonell RAL. Cortical hyperexcitability and epileptogenesis: understanding the mechanisms of epilepsy – Part 1. *J Clin Neurosci*. 2009; 16:355–65. [PubMed: 19124246]
3. Spencer SS. Neural networks in human epilepsy: evidence of and implications for treatment. *Epilepsia*. 2002; 43:219–27. [PubMed: 11906505]
4. Chang BS, Lowenstein DH. Mechanisms of disease: Epilepsy. *N Engl J Med*. 2003; 349:1257–66. [PubMed: 14507951]
5. Klingberg T, Hedehus M, Temple E, Salz T, Gabrieli JDE, Moseley ME, et al. Microstructure of temporo-parietal white matter as a basis for reading ability: evidence from diffusion tensor magnetic resonance imaging. *Neuron*. 2000; 25:493–500. [PubMed: 10719902]
6. Aghakhani Y, Kinay D, Gotman J, Soualmi L, Andermann F, Olivier A, et al. The role of periventricular nodular heterotopia in epileptogenesis. *Brain*. 2005; 128:641–51. [PubMed: 15659421]
7. Tassi L, Colombo N, Cossu M, Mai R, Francione S, Lo Russo G, et al. Electroclinical, MRI and neuropathological study of 10 patients with nodular heterotopia, with surgical outcomes. *Brain*. 2005; 128:321–37. [PubMed: 15618282]
8. Battaglia, G.; Granata, T. Periventricular nodular heterotopia. In: Sarnat, HB.; Curatolo, P., editors. *Handbook of Clinical Neurology*. Vol. 87. Amsterdam: Elsevier Inc; 2008. p. 177-89. (3rd series). *Malformations of the Nervous System*
9. Fox JW, Lamperti ED, Ekio lu YZ, Hong SE, Feng Y, Graham DA, et al. Mutations in filamin 1 prevent migration of cerebral cortical neurons in human periventricular heterotopia. *Neuron*. 1998; 21:1315–25. [PubMed: 9883725]
10. Chang BS, Ly J, Appignani B, Bodell A, Apse KA, Ravenscroft RS, et al. Reading impairment in the neuronal migration disorder of periventricular nodular heterotopia. *Neurology*. 2005; 64:799–803. [PubMed: 15753412]
11. Chang BS, Katzir T, Liu T, Corriveau K, Barzillai M, Apse KA, et al. A structural basis for reading fluency: white matter defects in a genetic brain malformation. *Neurology*. 2007; 69:2146–54. [PubMed: 18056578]
12. Archer JS, Abbott DF, Masterton RA, Palmer SM, Jackson GD. Functional MRI interactions between dysplastic nodules and overlying cortex in periventricular nodular heterotopia. *Epilepsy Behav*. 2010; 19:631–4. [PubMed: 21030316]
13. Christodoulou JA, Walker LM, Del Tufo SN, Katzir T, Gabrieli JDE, Whitfield-Gabrieli S, et al. Abnormal structural and functional brain connectivity in gray matter heterotopia. *Epilepsia*. 2012; 53:1024–32. [PubMed: 22524972]
14. Oldfield RC. The assessment and analysis of handedness: the Edinburgh inventory. *Neuropsychologia*. 1971; 9:97–113. [PubMed: 5146491]
15. Booth JR, Burman DD, Meyer JR, Gitelman DR, Parrish TB, Mesulam MM. Relation between brain activation and lexical performance. *Human Brain Mapp*. 2003; 19:155–69.
16. Booth JR, Burman DD, Meyer JR, Gitelman DR, Parrish TB, Mesulam MM. Development of brain mechanisms for processing orthographic and phonologic representations. *J Cogn Neurosci*. 2004; 16:1234–49. [PubMed: 15453976]
17. Misra M, Katzir T, Wolf M, Poldrack RA. Neural systems for rapid automatized naming in skilled readers: unraveling the RAN-reading relationship. *Scientific Studies of Reading*. 2004; 8:241–56.
18. Pugh KR, Shaywitz BA, Shaywitz SE, Constable RT, Skudlarski P, Fulbright RK, et al. Cerebral organization of component processes in reading. *Brain*. 1996; 119:1221–38. [PubMed: 8813285]
19. Brainard DH. The Psychophysics Toolbox. *Spatial Vision*. 1997; 10:433–6. [PubMed: 9176952]
20. Pelli DG. The VideoToolbox software for visual psychophysics: Transforming numbers into movies. *Spatial Vision*. 1997; 10:437–42. [PubMed: 9176953]
21. Wolf, M.; Denckla, MB. *Rapid Automatized Naming and Rapid Alternating Stimulus Tests (RAN/RAS)*. Austin, TX: Pro-Ed; 2005.

22. Thesen S, Hied O, Mueller E, Schad LR. Prospective acquisition correction for head motion with image-based tracking for real-time fMRI. *Magn Reson Med*. 2000; 44:457–65. [PubMed: 10975899]
23. Gorgolewski K, Burns CD, Madison C, Clark D, Halchenko YO, Waskom ML, et al. Nipype: A flexible, lightweight and extensible neuroimaging data processing framework. *Front Neuroinform*. 2011; 5:13. [PubMed: 21897815]
24. Dale AM, Fischl B, Sereno MI. Cortical surface-based analysis. I. Segmentation and surface reconstruction. *Neuroimage*. 1999; 9:179–94. [PubMed: 9931268]
25. Janszky J, Ebner A, Kruse B, Mertens M, Jokeit H, Seitz RJ, et al. Functional organization of the brain with malformations of cortical development. *Ann Neurol*. 2003; 53:759–67. [PubMed: 12783422]
26. McCandliss BD, Cohen L, Dehaene S. The visual word form area: expertise for reading in the fusiform gyrus. *Trends Cogn Sci*. 2003; 7:293–9. [PubMed: 12860187]
27. Nestor A, Behrmann M, Plaut DC. The neural basis of visual word form processing: a multivariate investigation. *Cereb Cortex*. 2013; 23:1673–84. [PubMed: 22693338]
28. Poldrack RA, Wagner AD, Prull MW, Desmond JE, Glover GH, Gabrieli JD. Functional specialization for semantic and phonological processing in the left inferior prefrontal cortex. *Neuroimage*. 1999; 10:15–35. [PubMed: 10385578]
29. Habib M. The neurological basis of developmental dyslexia: an overview and working hypothesis. *Brain*. 2000; 123:2373–99. [PubMed: 11099442]
30. Walker LM, Katzir T, Liu T, Ly J, Corriveau K, Barzillai M, et al. Gray matter volumes and cognitive ability in the epileptogenic brain malformation of periventricular nodular heterotopia. *Epilepsy Behav*. 2009; 15:456–60. [PubMed: 19541546]
31. Timofeev I, Bazhenov M, Avramescu S, Nita DA. Post-traumatic epilepsy: the roles of synaptic plasticity. *Neuroscientist*. 2010; 16:19–27. [PubMed: 19359668]
32. Chang BS, Walsh CA. Mapping form and function in the human brain: the emerging field of functional neuroimaging in cortical malformations. *Epilepsy Behav*. 2003; 4:618–25. [PubMed: 14698694]
33. Wagner J, Elger CE, Urbach H, Bien CG. Electric stimulation of periventricular heterotopia: participation in higher cerebral functions. *Epilepsy Behav*. 2009; 14:425–8. [PubMed: 19084612]
34. Galaburda AM, Sherman GF, Rosen GD, Aboitiz F, Geschwind N. Developmental dyslexia: four consecutive patients with cortical anomalies. *Ann Neurol*. 1985; 18:222–33. [PubMed: 4037763]
35. Hermann B, Meador KJ, Gaillard WD, Cramer JA. Cognition across the lifespan: antiepileptic drugs, epilepsy, or both? *Epilepsy Behav*. 2010; 17:1–5. [PubMed: 19931492]

Highlights

- We studied the functionality of nodular gray matter in periventricular heterotopia.
- We show that heterotopia are integrated into functional cortical circuits.
- Heterotopia activation is seen more commonly with tasks that are more challenging.
- This work helps us to understand how migration defects affect cerebral function.

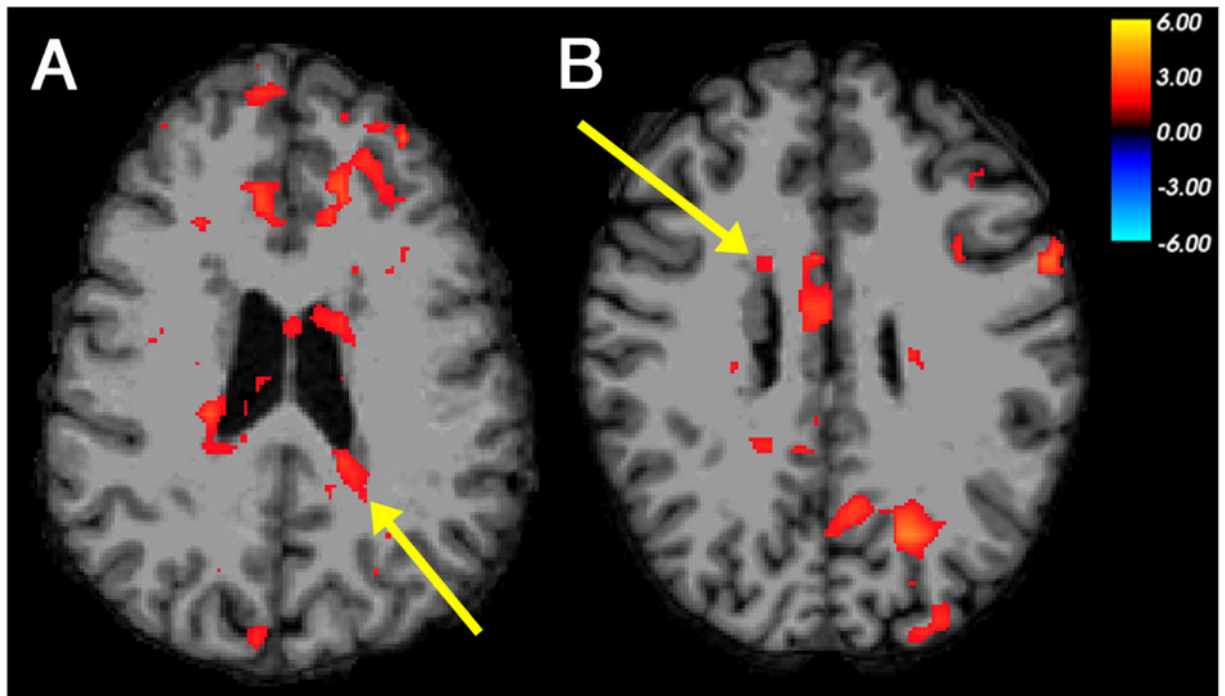


Figure 1. Co-activation of nodular heterotopia with multiple cortical regions in phonological processing

Examples of BOLD activation seen in periventricular nodules of gray matter and multiple regions of cerebral cortex, in a functional contrast between picture-mediated word rhyming and word matching judgments as performed by individuals with PNH. (A) Left posterior heterotopia activation (arrow), with co-activation in bilateral frontal cortex, in Participant 2. (B) Right frontal heterotopia activation (arrow), with co-activation in contralateral posterior cortex, in Participant 4. The color scale represents the t-statistic for a significant contrast at each voxel. The right side of the images represents the left side of the brains.

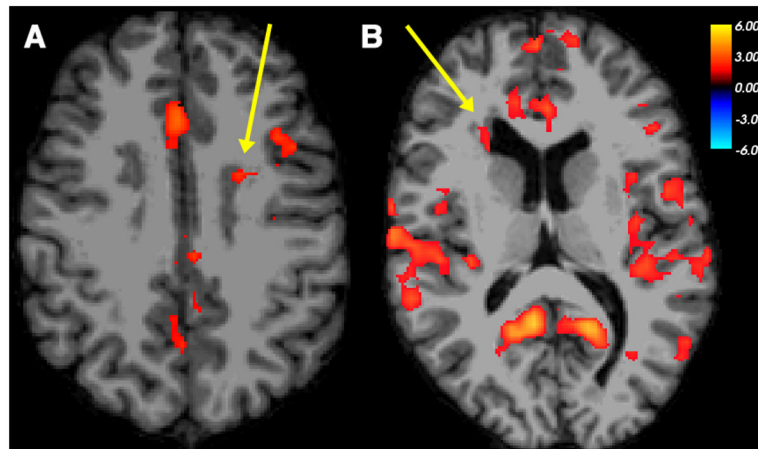


Figure 2. Co-activation of nodular heterotopia with overlying cortex and other cortical regions in orthographic processing

Examples of BOLD activation seen in periventricular nodules of gray matter and regions of cerebral cortex, in functional contrasts between word matching and control conditions as performed by individuals with PNH. (A) Left frontal heterotopia activation (arrow), with co-activation of overlying cerebral cortex in the left frontal lobe, in word matching > line matching contrast in Participant 1. (B) Right frontal heterotopia activation (arrow), with co-activation of multiple bilateral cortical regions, in word matching > symbol matching contrast in Participant 5. The color scale represents the t-statistic for a significant contrast at each voxel. The right side of the images represents the left side of the brains.

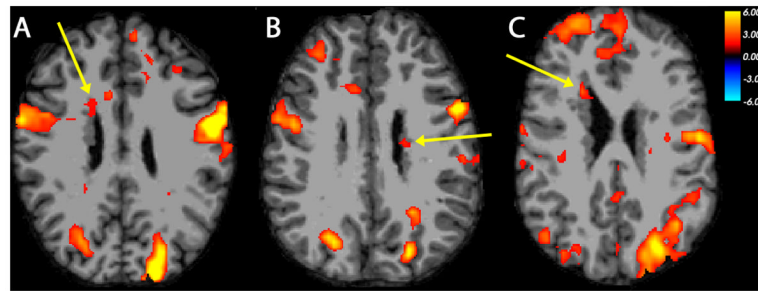


Figure 3. Co-activation of nodular heterotopia with overlying cortex and homologous contralateral cortex in RAN

Examples of BOLD activation seen in frontal periventricular nodules of gray matter and multiple regions of cerebral cortex, in functional contrasts between rapid silent naming and a rest condition as performed by individuals with PNH. (A) Right frontal heterotopia activation (arrow), with co-activation of overlying cortex and homologous contralateral region of cortex, during rapid letter naming task in Participant 4. (B) Left posterior frontal heterotopia activation (arrow), with similar co-activation, during rapid number naming task in Participant 6. (C) Right frontal heterotopia activation (arrow), with co-activation of overlying frontopolar cortex, during rapid two-set naming task in Participant 1. The color scale represents the t-statistic for a significant contrast at each voxel. The right side of the images represents the left side of the brains.

Table 1

Behavioral performance on reading-related tasks in periventricular nodular heterotopia participants

| fMRI Task | Percent accuracy, mean (SD) | Reaction time in msec, mean (SD) |
|-------------------------|-----------------------------|----------------------------------|
| Phonological | | |
| Picture-mediated | | |
| Word match | 98.75 (1.72) | 1625.75 (376.44) |
| Word rhyme | 84.58 (7.55) | 2258.37 (170.51) |
| Print-mediated | | |
| Word match | 97.92 (1.73) | 1396.68 (487.53) |
| Word rhyme | 90.00 (5.04) | 1715.66 (260.32) |
| Orthographic | | |
| Word match | 98.96 (2.95) | 1426.89 (675.63) |
| Lines match | 94.27 (8.31) | 1745.61 (647.31) |
| Symbols match | 93.23 (5.43) | 1910.16 (544.17) |
| RAN | | |
| Letters | | 3598.27 (797.25)* |
| Numbers | | 3629.07 (1057.29)* |
| Two-set | | 3949.32 (1003.46)* |

Abbreviations: SD = standard deviation; msec = milliseconds; RAN = rapid automatized naming

* For RAN tasks, time represents that required to complete silent reading of one line of the stimuli matrix.

Table 2
Functional activation within periventricular heterotopic nodules during performance of reading-related tasks

| Participant | Age (yr)/handed/sex | Phonological task contrasts | | | Orthographic task contrasts | | | Rapid naming task contrasts | | |
|-------------|---------------------|---|-----------------------|--|------------------------------|---|--|---|--|--|
| | | Picture rhyme vs. match | Print rhyme vs. match | Word match vs. lines match | Word match vs. symbols match | Letters vs. rest | Numbers vs. rest | Two-set vs. rest | | |
| 1 | 32/R/F | None | None | L anterior nodule, with overlying cortex (Fig. 2A) | None | None | None | None | R anterior nodule, with overlying and mult B cortical regions* (Fig. 3C) | |
| 2 | 42/R/M | L posterior nodule, with mult B cortical regions* (Fig. 1A) | None | None | None | L posterior nodule, with overlying and mult B cortical regions* | R anterior nodule, with overlying cortex* | None | None | |
| 3 | 27/R/F | None | None | None | None | None | None | None | None | |
| 4 | 27/R/F | R anterior nodule, with overlying and contra posterior cortex (Fig. 1B) | None | None | None | R anterior nodule, with overlying and contra homologous cortex* (Fig. 3A) | R anterior nodule, with overlying and contra homologous cortex* | R anterior nodule, with overlying and contra homologous cortex* | R anterior nodule, with overlying and contra homologous cortex* | |
| 5 | 29/R/F | None | None | None | None | R anterior nodule, with mult B cortical regions* (Fig. 2B) | None | None | None | |
| 6 | 21/R/M | None | None | None | None | None | L anterior nodule, with overlying and contra homologous cortex (Fig. 3B) | L anterior nodule, with overlying and contra homologous cortex | L anterior nodule, with overlying and contra homologous cortex | |
| 7 | 40/R/F | None | None | None | None | None | L and R posterior nodules, with mult B cortical regions* | L posterior nodule, with mult B cortical regions* | L posterior nodule, with mult B cortical regions* | |
| 8 | 19/R/F | None | None | None | None | None | None | None | None | |

Abbreviations: yr = years; L = left; R = right; F = female; M = male; B = bilateral; mult = multiple; contra = contralateral

* Cortical regions included those with demonstrated resting-state functional connectivity to indicated region of heterotopia as well [13].